Protein Science (2000), *9*:280–289. Cambridge University Press. Printed in the USA.

An interdomain distance in cardiac troponin C determined by fluorescence spectroscopy

WEN-JI DONG,[1] JOHN M. ROBINSON,[1] JUN XING,[1] PATRICK K. UMEDA,[2] AND HERBERT C. CHEUNG[1]

[1]Department of Biochemistry and Molecular Genetics, University of Alabama at Birmingham, Birmingham, Alabama 35294-2041
[2]Department of Medicine, University of Alabama at Birmingham, Birmingham, Alabama 35294-2041

(RECEIVED September 9, 1999; FINAL REVISION November 10, 1999; ACCEPTED November 12, 1999)

Abstract

The distance between Ca^{2+}-binding site III in the C-terminal domain and Cys35 in the N-terminal domain in cardiac muscle troponin C (cTnC) was determined with a single-tryptophan mutant using bound Tb^{3+} as the energy donor and iodoacetamidotetramethylrhodamine linked to the cysteine residue as energy acceptor. The luminescence of bound Tb^{3+} was generated through sensitization by the tryptophan located in the 12-residue binding loop of site III upon irradiation at 295 nm, and this sensitized luminescence was the donor signal transferred to the acceptor. In the absence of bound cation at site II, the mean interdomain distance was found to be 48–49 Å regardless of whether the cTnC was unbound or bound to cardiac troponin I, or reconstituted into cardiac troponin. These results suggest that cTnC retains its overall length in the presence of bound target proteins. The distribution of the distances was wide (half-width >9 Å) and suggests considerable interdomain flexibility in isolated cTnC, but the distributions became narrower for cTnC in the complexes with the other subunits. In the presence of bound cation at the regulatory site II, the interdomain distance was shortened by 6 Å for cTnC, but without an effect on the half-width. The decrease in the mean distance was much smaller or negligible when cTnC was complexed with cTnI or cTnI and cTnT under the same conditions. Although free cTnC has considerable interdomain flexibility, this dynamics is slightly reduced in troponin. These results indicate that the transition from the relaxed state to an activated state in cardiac muscle is not accompanied by a gross alteration of the cTnC conformation in cardiac troponin.

Keywords: cardiac troponin C; energy transfer; terbium

Force generation in vertebrate striated muscle is triggered by the binding of Ca^{2+} to the regulatory sites of troponin C. The Ca^{2+} signal is believed to be transmitted to the other proteins of the thin filament via a strong Ca^{2+}-dependent interaction between TnC and TnI within the three-subunit troponin complex. This interaction weakens the interaction between TnI and actin, relieves the inhibitory effect of TnI on actomyosin ATPase in relaxed muscle, and thus activates the ATPase and initiates the contractile cycle. TnC from fast skeletal muscle contains four metal ion binding sites, designated as sites I and II in the N-terminal domain and sites III and IV in the C-terminal domain. Sites III and IV have a relatively high affinity for Ca^{2+} ($K_a \sim 10^7\ M^{-1}$) and bind Mg^{2+} competitively ($K_a \sim 10^3\ M^{-1}$). Sites I and II are specific for Ca^{2+} and have a low affinity ($K_a \sim 10^5\ M^{-1}$). Several lines of evidence indicate that sites I and II are the regulatory sites of the contractile cycles and sites III and IV play a structural role with no known function.

The crystal structure of avian fsTnC shows a dumbbell-shaped molecule with the N- and C-terminal segments each folded into two globular domains connected by a 22-residue α-helix. The length of the molecule in the crystal structure is about 75 Å (Herzberg & James, 1985; Sundaralingam et al., 1985). Each metal ion binding site is formed by a helix-loop-helix EF-hand motif in which the cation is coordinated to the 12-residue loop, and the two flanking helices are orientated at an angle close to 90°.

The amino acid sequence of cardiac muscle TnC is 70% identical to that of fsTnC, and the Ca^{2+} binding site I in cTnC is inactive in coordinating Ca^{2+} due to substitutions of two critical amino acids and an insertion in the binding loop. Thus, cTnC has only one regulatory site for Ca^{2+} and this single site is sufficient

Reprint requests to: H.C. Cheung, Department of Biochemistry and Molecular Genetics, University of Alabama at Birmingham, Birmingham, Alabama 35294-2041; e-mail: hccheung@uab.edu.

Abbreviations: Tn, troponin; cTn, cardiac muscle troponin; TnC, troponin C; fsTnC, fast skeletal TnC; cTnC, cardiac troponin C; cTnI, cardiac troponin I; cTnT, cardiac troponin T; Y111W, cTnC mutant C84S/Y111W; R147W, cTnC mutant C84S/R147W; Y111W/R147W, cTnC mutant C84S/Y111W/R147W; FRET, fluorescence resonance energy transfer; DTT, dithiothreitol; MOPS, 3-(*N*-morpholino)propanesulfonic acid; EGTA, ethylene glycol-bis-(β-aminoethyl ether)-*N,N,N′,N′*-tetraacetic acid; IAATMR, 5- and 6-iodoacetamidotetramethylrhodamine; IAANS, 2-[4′-(iodoacetamido) anilino]naphthalene-6-sulfonic acid.

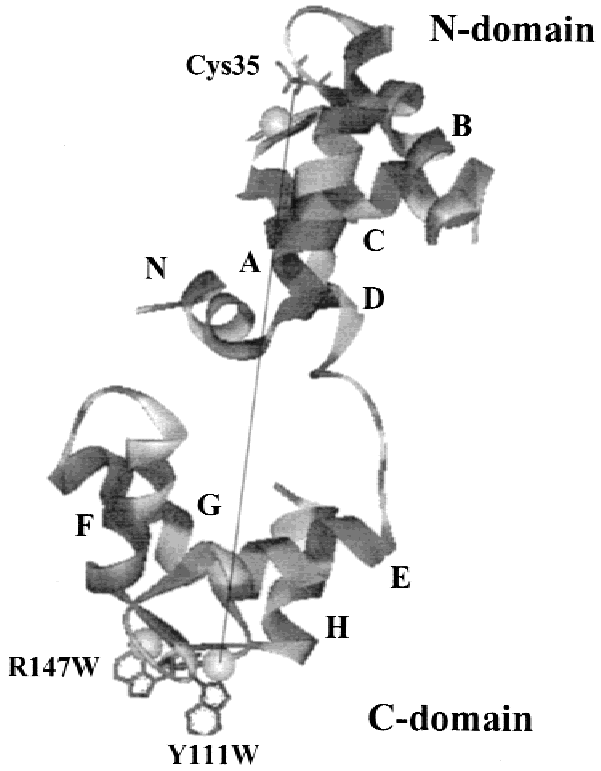

Fig. 1. A ribbon model of holo cTnC based on the NMR structure (Sia et al., 1997 and PDB IAJ4). The relative orientations of the two domains and the structure of the central helix are undefined because of the flexibility of the central helix in solution. The N-terminal domain has five helices (N and A–D), and the C-domain has four helices (E–H). The structure of the N-domain contains one bound Ca^{2+} (sphere) at site II, and that of the C-domain contains two bound Ca^{2+} at sites III and IV. Cys35 is within the Ca^{2+} binding loop of site I, which is inactive in coordinating the cation. Also indicated in the structure are two residues (Tyr111 and Arg147) that were mutated to tryptophan and the tryptophan mutants were studied in this work. The orientations of the two domains were adjusted to yield a distance of 48 Å from Cys35 to the bound cation at site III shown adjacent to the indole ring of Y111W.

to regulate contraction in cardiac muscle. The crystal structure of cTnC is not available, but its solution NMR structure has been reported recently and is shown in Figure 1. There are substantial differences in the conformations of the N-domain in both the apo and holo states between fsTnC and cTnC, as recently shown by NMR (Sia et al., 1997) and FRET studies (Dong et al., 1999). The central helix of cTnC in solution is flexible and has an undefined NMR structure. No information is available as to whether this flexibility is significantly modified when cTnC is reconstituted into troponin. Such information is essential for an understanding of the role of structural dynamics of cTnC in Ca^{2+} activation and may provide insights into design of pharmaceutical agents targeted to cTnC.

Early studies showed that trivalent lanthanide ions bind to TnC in competition with Ca^{2+} at all four sites (Leavis et al., 1980; Wang et al., 1981). The addition of Tb^{3+} to fsTnC at a stoichiometry of 2:1 or less resulted in saturation of only the two high-affinity sites in the C-domain (Leavis et al., 1980; Wang et al., 1982). Peptides of 12 amino acids or longer based on the loop of the Ca^{2+}-binding site II of fsTnC in which a phenylalanine was replaced by tyrosine enhanced the luminescence of bound Tb^{3+} upon irradiation at 276 nm, suggesting an energy transfer from the aromatic residue to the bound lanthanide ion (Kanellis et al., 1983; Malik et al., 1987). In a study of 14 oligopeptides based on a consensus sequence of the metal-binding loops from the calmodulin family, it was shown that tryptophan in the seventh position of the loop was more efficient in enhancing Tb^{3+} luminescence than aromatic residues in other positions (MacManus et al., 1990). The luminescence of the 545 nm Tb^{3+} band has an extensive spectral overlap with the absorption spectrum of tetramethylrhodamine with a Förster critical distance about 60 Å (Selvin & Hearst, 1994). In the present work, we used a cTnC mutant in which the endogenous tyrosine at position seven in the binding loop of site III in the C-domain was replaced with a tryptophan, which served to sensitize the luminescence of Tb^{3+} bound to this site. This sensitized Tb^{3+} luminescence was used as the donor of resonance energy transfer to Cys35 labeled with IAATMR. The FRET data of the Tb^{3+}-IAATMR pair were analyzed to determine the distribution of the interdomain distances in several conditions. This distance is not affected by reconstitution of cTnC into cardiac troponin.

Results

Characterization of cTnC mutants

The three tryptophan-containing cTnC mutants are Y111W, R147W, and Y111W/R147W. In addition to tryptophan, each mutant contained a single endogenous cysteine (Cys35) with the other cysteine (Cys84) replaced by serine. They were assayed for their ability to regulate myofibrillar ATPase activity. This was done with myofibrils prepared from fresh rat hearts. The myofibrils were first depleted of endogenous cTnC, followed by reconstitution with an exogenous cTnC. The Ca^{2+}-activated ATPase activities of the preparations reconstituted with cTnC mutants were greater than 82% of the activity of a control which was reconstituted with wild-type cTnC (specific activity 161 nmol Pi/min/mg myofibril protein). These ATPase activities were within the range of activities for cardiac myofibrils, and these results indicated that the mutations did not alter the mutants' functional property to any significant extent.

Figure 2 shows the fluorescence emission spectra of the three mutants, and the spectral parameters are listed in Table 1. Trp111 in Y111W is in the binding loop of site III, and its fluorescence was sensitive to the binding of both Mg^{2+} and Ca^{2+}. The two cations had opposite effects on the spectrum: Mg^{2+} induced a small blue spectral shift and Ca^{2+} elicited a 4 nm red-shift indicating a more polar tryptophan environment in the presence of bound Ca^{2+}. The effects of Mg^{2+} and Ca^{2+} had similar effects on the environment of the tryptophan R147W in site IV: the binding of both cations inducing a red spectral shift indicating a more polar environment in the presence of these bound cations. The pattern of changes induced by the two cations on the lifetimes (Table 1) of individual tryptophans was consistent with that observed for the steady-state spectroscopic parameters. The more polar environments in the presence of bound Ca^{2+} suggested by the spectral shifts were due to a small increase in solvent accessibility as demonstrated by the second-order constant of acrylamide quenching. In the absence of bound Ca^{2+}, the quenching constants for Y111W and R141W were $1.47 \times 10^9\ M^{-1}\ s^{-1}$ and $1.41 \times 10^9\ M^{-1}\ s^{-1}$, respectively. In the presence of bound Ca^{2+}, these constants increased to $2.05 \times 10^9\ M^{-1}\ s^{-1}$ and $2.78 \times 10^9\ M^{-1}\ s^{-1}$. The

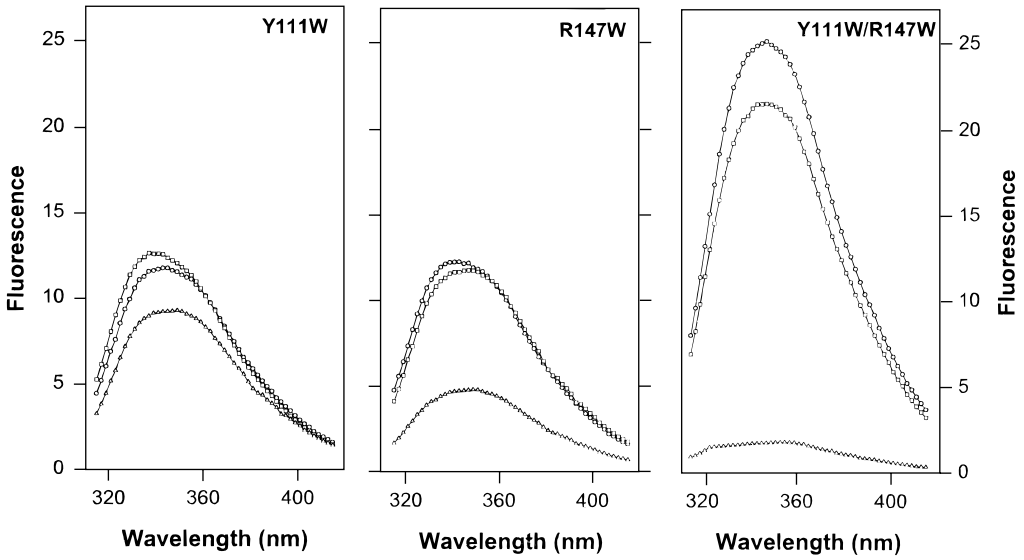

Fig. 2. Fluorescence emission spectra of tryptophan-containing cTnC mutants, excitation 295 nm. Samples contained 5 μM protein in buffer A containing 1 mM EGTA. Circles: no added cation; squares: in the presence of 5 mM Mg^{2+}; and triangle: 5 mM Mg^{2+} + 3 mM Ca^{2+}.

twofold increase in the quenching constant indicates an increased exposure of the tryptophan to the solvent and accounts for the observed Ca^{2+}-induced red-shift of the emission spectrum. The emission of Trp111 and Trp147 in the double-tryptophan mutant was different from that of either tryptophan alone. The composite fluorescence emission spectra was red-shifted compared with the spectra of individual tryptophans. The overall emission was highly quenched as indicated by the very small apparent quantum yield and short mean lifetime.

Sensitized luminescence spectra of Tb^{3+} bound to cTnC mutants

A set of steady-state fluorescence emission spectra of mutant Y111W in the presence of increasing concentration of Tb^{3+} is shown in Figure 3. The tryptophan emission band at 335 nm was progressively quenched with the appearance of the three Tb^{3+} luminescence bands at 480, 545, and 585 nm. The reciprocal changes in the tryptophan and the lanthanide bands with increasing $[Tb^{3+}]$ indicate an efficient energy transfer from donor tryptophan to Tb^{3+} bound at site III. To rule out the possibility that the large tryptophan quenching was due to structural changes induced by Tb^{3+} rather than an energy transfer, Tb^{3+} was replaced by Gd^{3+} in a separate experiment. Although the two lanthanide ions are expected to have similar binding properties toward cTnC, no large quenching was observed by Gd^{3+} (data not shown), indicating no energy transfer to bound Gd^{3+}. The latter result was expected because of the large energy gap between the ground state and the first excited state in Gd^{3+} and showed that the observed tryptophan quenching by Tb^{3+} was due to an energy transfer.

Table 1. *Tryptophan fluorescence parameters of cTnC mutants*

Mutant[a]	Condition[b]	λ_{max} (nm)	Q	Decay time[c] (ns)		$\langle\tau\rangle$[d] (ns)
				τ_1	τ_2	
Y111W	EGTA	345	0.32	2.05 (0.40)	5.19 (0.60)	4.54
	Mg^{2+}	342	0.34	2.42 (0.59)	5.41 (0.41)	4.24
	Ca^{2+}	349	0.25	1.94 (0.56)	4.39 (0.44)	3.48
R147W	EGTA	343	0.26	1.98 (0.43)	5.05 (0.57)	4.43
	Mg^{2+}	347	0.26	1.57 (0.19)	5.26 (0.81)	5.02
	Ca^{2+}	350	0.11	1.2 (0.60)	2.87 (0.40)	2.23
Y111W/R147W	EGTA	347	0.29	2.20 (0.34)	5.44 (0.66)	4.88
	Mg^{2+}	349	0.24	1.47 (0.29)	4.54 (0.81)	4.32
	Ca^{2+}	355	0.024	0.48 (0.02)	3.49 (0.98)	3.48

[a]The mutants each also contained an additional mutation: Cys84 $\rightarrow$ Ser.
[b]Mg^{2+}: samples were in buffer A containing 1 mM EGTA and 5 mM Mg^{2+}; Ca^{2+}: samples in buffer A containing 1 mM EGTA, 5 mM Mg^{2+}, and 3 mM Ca^{2+}.
[c]The numbers in parentheses are the fractional amplitudes (α_i) associated with each lifetime τ_i.
[d]$\langle\tau\rangle$ is the intensity-weighted mean lifetime calculated from $\langle\tau\rangle = \sum\alpha_i\tau_i^2/\sum\alpha_i\tau_i$.

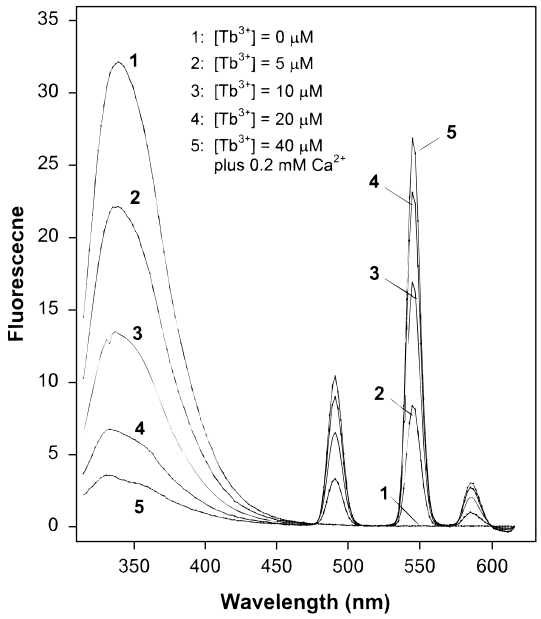

Fig. 3. Luminescence spectra of Tb^{3+} bound to cTnC mutant Y111W and sensitized by Trp111 at the binding site. The tryptophan was excited at 295 nm. Samples contained 5 μM protein in buffer A containing 10 μM EGTA and 5 mM Mg^{2+}. The concentration of Tb^{3+} varied from 0 to 40 μM, as indicated in the figure. The three Tb^{3+} bands have peaks at 480, 545, and 585 nm.

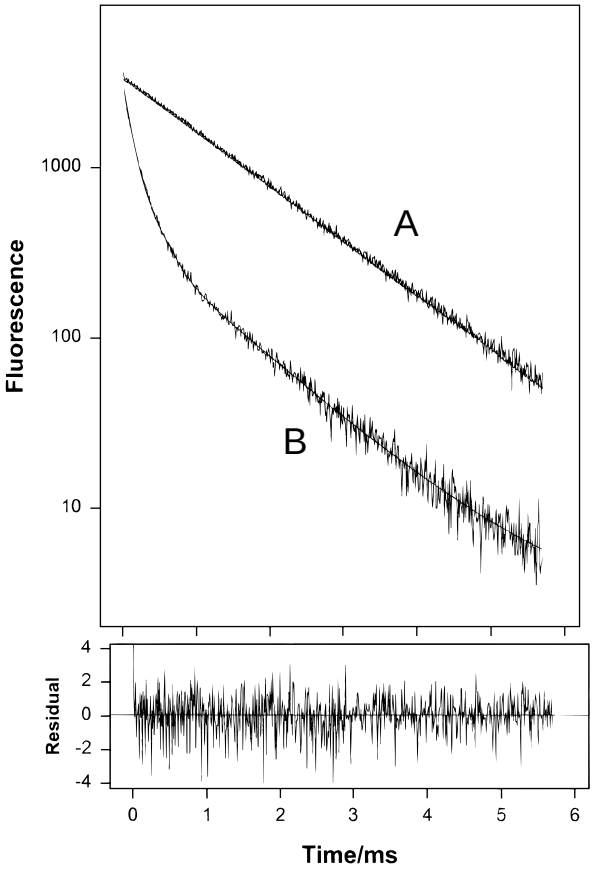

Fig. 4. Representative luminescence intensity decay curves of bound Tb^{3+} at site III of cTnC mutant Y111W. **A:** The single-exponential decay of the bound Tb^{3+} in the absence of an energy acceptor (lifetime 1.51 ms). **B:** The Tb^{3+} decay determined in the presence of the acceptor AATMR attached to Cys35; the tracing was fitted to the sum of two exponential terms with lifetimes 0.37 ms (amplitude 0.77) and 1.41 ms (amplitude 0.23). The bottom panel shows the residual plot of the two-exponential fit of the decay data shown in **B**. The excitation wavelength was 295 nm, and the sensitized Tb^{3+} luminescence was detected at 545 nm. Samples contained 5 μM protein in buffer A and 10 μM Tb^{3+}, 2 μM EGTA, and 5 mM Mg^{2+}.

The decay of the sensitized luminescence intensity of Tb^{3+} bound to Y111W at 545 nm is shown in Figure 4 (top curve). The decay was single exponential with a lifetime of 1.51 ms. The lifetime was increased to 3.01 ms when the decay measurement was carried out in D_2O. The difference of the lifetime in the two solvents allowed calculation of the number of water molecules bound to the inner coordination sphere of Tb^{3+} at site III from the following relationship (Horrocks & Sudnick, 1979): number of water molecule $= A[(1/\tau(H_2O) - 1/\tau(D_2O)]$, where A is a constant and is equal to 4.2 for Tb^{3+}, and τ is the lifetime in H_2O or D_2O. The lifetime data yielded 1.4 bound waters/Tb^{3+}.

The presence of H_2O in the inner coordination sphere of Tb^{3+} bound to Y111W contributed to the nonradiative de-excitation process and, therefore, a reduced quantum yield. From the ratio of the two lifetimes determined in H_2O and D_2O, the quantum yield of bound Tb^{3+} was calculated to be 0.5. Table 2 lists these luminescence properties of bound Tb^{3+} for all three cTnC mutants and these mutants bound to cTnI and cTnI plus cTnT. The presence of the other two subunits did not alter the luminescence properties of Tb^{3+} bound to cTnC mutants. Since wild-type cTnI and native cTnT used to form complexes with cTnC mutants contain endogenous tryptophans, it was necessary to rule out any potential effects these tryptophans might have on the sensitized bound Tb^{3+} luminescence. An experiment was performed using Tb^{3+} bound to cTn reconstituted from wild-type subunits in which cTnC contained no tryptophan at site III. No sensitized Tb^{3+} luminescence was detected from the reconstituted sample upon irradiation at 295 nm, indicating that the tryptophans of cTnI and cTnT in cTn are located beyond the range of energy transfer to bound Tb^{3+} at the site III of cTnC.

Determination of an interdomain distance in cTnC

Of the three cTnC mutants studied, mutant Y111W exhibited the largest sensitized Tb^{3+} luminescence intensity and the longest decay time. This mutant was selected as a model system to determine the distance between Tb^{3+} bound to site III (donor) and Cys35 labeled with IAATMR (acceptor) in the N-domain. Since all three sites bind Tb^{3+}, we determined the affinities of the sites of the mutant for Tb^{3+} and Ca^{2+} in order to optimize conditions for FRET measurements. Table 3 lists the binding constants of the two sets of sites for both cations. For the single regulatory site in the N-domain, the binding constant of Tb^{3+} was 16-fold larger than that of Ca^{2+}. The affinity of Tb^{3+} at the C-domain sites (sites III and IV) was 14 times higher than that at the N-domain site, and this affinity was increased two fold when cTnC was reconstituted into either the binary cTnC-cTnI complex or the ternary complex with both cTnI and cTnT. These results enabled us to use a low [Tb^{3+}] (relative to [cTnC]) so that only a fraction of the sites III and IV was saturated, leaving the regulatory site unoccupied by

Table 2. *Luminescence parameters of Tb^{3+} bound to cTnC mutants*

Sample[a]	τ in H_2O (ms)	τ in D_2O (ms)	Quantum yield	H_2O molecule[b]	Relative brightness[c]
Y111W	1.51	3.01	0.50	1.4	1.0
+ cTnI	1.54	3.02	0.51	1.3	1.1
+ cTnI + cTnT	1.52	3.02	0.50	1.4	1.0
R147W	1.38	3.00	0.46	1.6	0.71
+ cTnI	1.40	3.01	0.47	1.6	0.73
+ cTnI + cTnT	1.41	3.01	0.47	1.6	0.72
Y111W/R147W	1.32	3.01	0.44	1.8	0.53
+ cTnI	1.34	3.01	0.45	1.7	0.55
+ cTnI + cTnT	1.33	3.02	0.44	1.8	0.56

[a]The three cTnC mutants are the same as those listed in Table 1. The luminescence properties of Tb^{3+} bound to the mutants were measured with individual mutants and with each mutant in the presence of cTnI and cTnI plus cTnT in a buffer containing Tb^{3+} and no added divalent cation.

[b]This is the number of water molecules coordinated to the inner sphere of Tb^{3+} bound to its sites in cTnC mutants.

[c]The brightness of bound Tb^{3+} is the total sensitized luminescence intensity at all wavelengths in the steady-state luminescence spectrum. The total intensity of bound Tb^{3+} of each sample was normalized to the total intensity of mutant Y111W.

Tb^{3+}. The distance determined between bound Tb^{3+} at site III and AATMR-Cys35 under this condition was the interdomain distance with an apo N-domain. It would be possible to obtain a holo cTnC fully saturated with Tb^{3+} at all three sites by the addition of a large excess of the lanthanide, but the excess and unbound Tb^{3+} would form insoluble hydroxide at physiological pH. To avoid this undesirable side effect, we added only a moderately large $[Tb^{3+}]$ plus 0.2 mM Ca^{2+} such that site II would be occupied by either Tb^{3+} or Ca^{2+} and a large fraction of sites III and IV would still be occupied by Tb^{3+}. This strategy enabled us to determine an interdomain distance in cation-loaded cTnC.

A typical Tb^{3+} decay curve determined in the presence of the acceptor is shown in Figure 4 (lower curve). The presence of a short component with a lifetime of 0.37 ms was due to an energy transfer and the long component of 1.41 ms reflected unquenched donor luminescence. In a separate experiment with the same sample, we measured the decay of the sensitized AATMR fluorescence emission intensity and found a dominant component with a lifetime of 0.37 ms (data not shown), in agreement with the decay of the quenched donor signal. This agreement confirms that the change in the decay time of bound Tb^{3+} reflected accurately an energy transfer between the sites in the two cTnC domains. Since both sites III and IV bind Tb^{3+}, the observed Tb^{3+} signal could contain a contribution from the lanthanide ion bound to site IV. This contribution was unlikely because the signal of bound Tb^{3+} was generated through sensitization by Trp111 located in site III. The Förster distance for the Trp-Tb^{3+} pair is <4 Å (Horrocks & Collier, 1981) and any sensitization of Tb^{3+} luminescence at site IV by Trp111 would be negligible or small.

Table 3. *Binding constants of cTnC(Y111W) for Ca^{2+} and Tb^{3+}*

Cation	N-domain[a] (Site II)	C-domain[b] (Sites III and IV)
Ca^{2+}	2.73×10^5	
Tb^{3+}	4.47×10^6	6.56×10^7 (1.73×10^8)[c] (1.69×10^8)[d]

[a]The constants for the single regulatory site II were determined with the mutant labeled with the extrinsic probe IAANS at Cys84. The change in the probe fluorescence recorded during titration experiments with Ca^{2+} or Tb^{3+} was used to determine the binding constants. The probe at Cys84 is known to monitor cation binding only to site II and not to the other sites (Dong et al., 1997c).

[b]The Tb^{3+} binding constant was determined from the quenching of the Trp111 fluorescence upon irradiation at 295 nm.

[c]Determined with the cTnC-cTnI complex obtained from the cTnC mutant and wild-type cTnI.

[d]Determined with cardiac troponin reconstituted from the cTnC mutant and the other two subunits (cTnI and cTnT).

Figure 5A shows a series of the luminescence intensity decay curves of Tb^{3+} bound to site III for isolated cTnC mutant Y111W. In the presence of both Tb^{3+} and Ca^{2+} (regulatory site II saturated), the quenching of Tb^{3+} intensity (bottom curve, blue) was faster than in the presence of a low $[Tb^{3+}]$ (second curve from top, red). This faster decay suggested an increase in energy transfer and a decrease in the interdomain separation. This change was not evident in the decay curves for the cTnC-cTnI complex (Fig. 5B) or the fully reconstituted troponin (Fig. 5C). These FRET data were analyzed in terms of a distribution of the distances between the two domains, and the distribution curves are displayed in Figure 6. The recovered distance parameters are listed in Table 4.

For cTnC with an apo N-domain (low $[Tb^{3+}]$), the distance appeared to remain in the range 48–49 Å regardless of whether cTnC was free or in the binary or ternary complex. However, the distribution was wide with a large half-width (>9 Å) for unbound cTnC and was narrower (half-width 6–7 Å) for cTnC in the complexes. The wide distribution may reflect a flexible central helix and the narrower distributions of the complexes suggested some constraint in this flexibility. For isolated cTnC fully saturated with cations (high $[Tb^{3+}]$ plus Ca^{2+}, Fig. 6A), the distribution was shifted to shorter distances, leaving the half-widths essentially un-

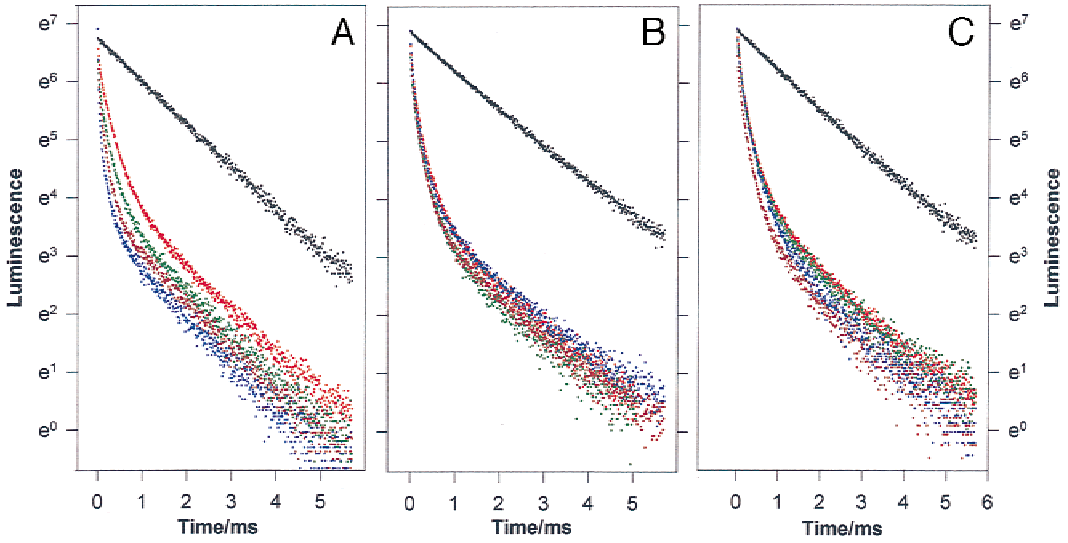

Fig. 5. Luminescence decay of Tb^{3+} bound to cTnC mutant Y111W labeled with IAATMR at Cys35 and in the presence of the other troponin subunits. **A:** cTnC mutant alone. **B:** cTnC in the presence of cTnI (cTnC-cTnI). **C:** cTnC reconstituted into cTn. Also included in each panel is the decay of the donor-alone sample in which the Cys35 was not labeled with the acceptor (black). Ratio of $[Tb^{3+}]$/[protein]: 0.4 (red), 1.0 (dark green), 2.0 (dark red), and 3.0 + 0.2 mM Ca^{2+} (blue). Other conditions were the same as given in Figure 4.

changed. This decrease in $\bar{r}$ induced by saturation of the single site in the N-domain was large for unbound cTnC (6 Å), smaller for cTnC-cTnI (2.5 Å), and negligible for the ternary complex. Thus, in the presence of bound cation in the N-domain, there was a 4 Å increase in the distance when cTnC was reconstituted into the complexes and the presence of the other two bound subunits appeared to impose a constraint on the global conformation of cTnC.

We evaluated the range of the mean distances consistent with the data that yielded the two distributions for isolated cTnC shown in Figure 6A. This was accomplished by calculating the χ_R^2 surfaces for the two mean distances as in previous work (Lakowicz et al., 1988; She et al., 1998). The two surfaces intersected at a χ_R^2 value 3.0-fold higher than the minimum value and >2.9-fold higher than the value with random noise in 68% of repetitive measurements. This analysis showed that the two distributions were distinct and the two mean distances were significantly different. Similar analyses were performed on the distributions for the binary and ternary complexes of cTnC (Fig. 6B,C). The two χ_R^2 surfaces for the $\bar{r}$ values of the two distributions in each figure intersected near the minimum value of χ_R^2, indicating that two distributions could not be distinguished. A comparison of the surfaces for the $\bar{r}$ values of the three distributions determined in the absence of bound cation in the N-domain (closed circles, Fig. 6A–C) indicated that all three distributions were indistinguishable by the data. Finally, the two distributions determined in the presence of bound cation at the N-domain in cTnC-cTnI and cTn (Fig. 6B,C, open circles) are superposable with essentially identical values for $\bar{r}$. Thus, the mean value of the interdomain distance of cTnC in the absence of bound cation in the regulatory domain was the same regardless of whether cTnC was free or complexed with the other subunits. This distance in the complexes was not affected by the presence of bound cation at the regulatory N-domain.

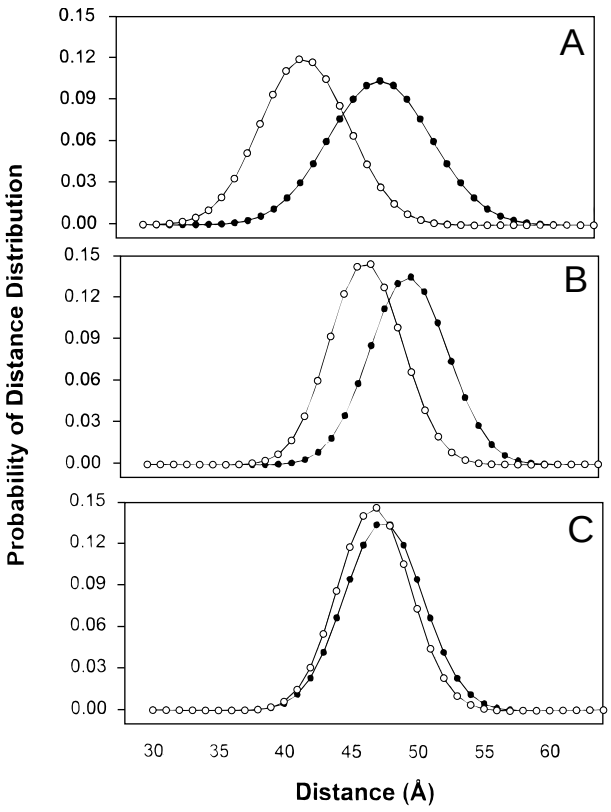

Fig. 6. Distribution of the distances between bound Tb^{3+} at site III and Cys35 at the inactive site I of cTnC mutant Y111W. **A:** cTnC alone. **B:** cTnC-cTnI. **C:** Reconstituted cTn. Closed circles, low $[Tb^{3+}]$ (N-domain site II unoccupied); open circles, high $[Tb^{3+}]$ + Ca^{2+} (site II occupied).

Table 4. *Distribution of the interdomain distances between Cys35 and site III in cTnC*[a]

	cTnC		cTnC-cTnI		cTnC-cTnI-cTnT	
[Tb^{3+}]/[protein]	$\bar{r}$ (Å)	*hw* (Å)	$\bar{r}$ (Å)	*hw* (Å)	$\bar{r}$ (Å)	*hw* (Å)
0.25	48.0	9.4	49.2	6.9	47.8	6.2
0.50	47.2	9.3	48.6	6.5	47.4	6.1
0.75	46.9	8.9	48.1	5.9	48.2	6.3
1.0	46.6	10.0	48.6	6.5	47.6	6.4
1.5	45.2	9.3	47.1	6.1	46.4	6.7
2.0	44.2	9.3	47.1	6.5	46.3	6.8
2.6	42.1	8.8	46.7	6.4	46.8	6.4
3.0[b]	42.3	8.8	46.7	6.6	47.0	6.4

[a]Measurements were carried out with [protein] = 5 μM in buffer A containing 2 μM EGTA and 5 mM Mg^{2+}.
[b]This sample also contained 0.2 mM Ca^{2+} so that the single low-affinity site II in cTnC was saturated with either Tb^{3+} or Ca^{2+}.

Discussion

Many biophysical studies of TnC have been made with an isolated protein. Since TnC does not function in isolation of the other two subunits, it is necessary to examine its structural features in complexes with either TnI or both TnI and TnT. The present study was undertaken to establish the extent to which cardiac TnC may experience a global conformational change within the troponin complex. The main structural information reported here is the distribution of the distances between two specific sites, one located in the N-domain and the other in the C-domain and separated by about 49 Å in the absence of bound activator Ca^{2+} at the N-domain.

The coordination of cation by EF-hand motifs involves 6 of the 12 residues within the 12-residue binding loop. The residue at the seventh position ($-y$ coordinating position) is involved in coordination via its main-chain carbonyl oxygen rather than the side-chain carboxylate oxygen. This residue was previously replaced by tryptophan in all four sites of calmodulin, and the replacement was shown not to distort the Ca^{2+}-binding site geometry and not to interfere with coordination of the main-chain C=O of this residue to Ca^{2+} (Chabbert et al., 1991). We replaced the endogenous residues in the seventh position in sties III (mutant Y111W) and IV (mutant R147W) of cTnC for FRET studies between Cys35 and the C-domain, using Tb^{3+} as a Ca^{2+} replacement. We also generated a third mutant containing the double mutations (Y111W/R147W) and studied its emission properties.

We used two separate energy transfer processes to determine the distance between site III and Cys35. The first is sensitization of bound Tb^{3+} luminescence by irradiation of the tryptophan at the binding site. The sensitized Tb^{3+} luminescence serves as an energy donor to an acceptor probe linked to Cys35. The use of sensitized Tb^{3+} luminescence rather than direct excitation of the lanthanide ion has two advantages. A powerful laser is required for direct excitation of Tb^{3+} luminescence, but not for irradiation of tryptophan to sensitize Tb^{3+} luminescence. A pulsed xenon lamp is adequate for this sensitization and was used in this study. Since both sites III and IV likely bind Tb^{3+} with an equal affinity, there is no easy way to selectively excite the bound ion at one site and not the bound ion at the other site by direct excitation. This problem is circumvented in the present approach because the tryptophan located at site III is likely beyond the range over which its excitation energy can be transferred to Tb^{3+} bound to site IV, and vice versa.

The tryptophans in the two cTnC mutants are located in equivalent positions in both sites III and IV and are useful for sensing structural changes induced by Mg^{2+} and Ca^{2+} at these sites. In the absence of any divalent cation, the two tryptophans have slightly different spectroscopic properties that reflect a small difference in the sequences of the two loops. Trp111 at site III has an unusually high quantum yield and this value is 23% higher than that observed for Trp147 at site IV. The binding of Mg^{2+} to both sites induces relatively minor spectroscopic changes, but the binding of Ca^{2+} elicits spectral changes that clearly suggest a more polar environment of both tryptophans. The changes are more pronounced for site IV than site III as indicated by changes in both the quantum yield and the mean lifetime. The Trp147 at site IV is more highly quenched by bound Ca^{2+} than the Trp111 at site III. This difference in quenching may be related to the small difference in the number of water molecules bound to the inner coordination sphere of Tb^{3+} at the two sites (1.4 vs. 1.6 waters for Tb^{3+} at site III and site IV, respectively). This interpretation is consistent with a general trend shown in Table 2 for the mutants in complexes with the other troponin subunits. The composite properties of the two tryptophans in the double mutant Y111W/R147W also suggest an overall more polar environment for both tryptophans in the Ca^{2+} complex. We examined the energy minimized structure of the double-tryptophan mutant containing bound Ca^{2+} at both sites III and IV. The centers of the two indole rings are about 4 Å apart, with the two rings facing each other and oriented at an angle less than 90°. This orientation and the short separation can lead to self-quenching of the fluorophores, giving rise to the observed large quenching of the tryptophan fluorescence.

The enhancement of Tb^{3+} luminescence upon binding to the cTnC mutants provides a convenient donor signal for FRET measurement with the AATMR probe. The bound Tb^{3+} serves as a pseudo-intrinsic probe for structural/functional changes of cTnC. An early study reported a distance of 34 Å for the transfer of energy from bound Tb^{3+} at both sites III and IV to a probe attached to both Cys35 and Cys84 (Wang & Leavis, 1990). This distance is much shorter than the distance between two specific sites reported here, but consistent with our result. Cys84 is located at the C-terminal end of helix D and considerably closer to the C-domain than Cys35 (Fig. 1). This shorter distance was weighted more heavily than the longer distance to Cys35 because of the inverse sixth power dependence of energy transfer on distance, and the energy transfer observed from the C-domain sites to the two

cysteines contained a larger contribution from the shorter distance. The overall effect is that the apparent distance must be much shorter than the longer distance.

As an initial model, the crystal structure of skeletal TnC is frequently used to describe the properties of cTnC in solution. This structure gives a distance of 56 Å between the site III and site I. The recent NMR structure of holo cTnC does not address this distance because the structure of the flexible central helix is undefined. The FRET data give a wide distribution of the distances between the two sites with the mean distance of 48 Å for cTnC without bound Ca^{2+} at the regulatory site in the N-domain. The determination of this mean interdomain distance is independent of the nature of the flexible central helix. The wide distribution, however, is consistent with an appreciable structural dynamics between the two domains. The significant finding is that the mean interdomain distance is not affected when cTnC is reconstituted into the cTnC-cTnI complex or the three-subunit troponin complex. This conclusion is strengthened by the fact that the donor probe is Tb^{3+}, which decays into multiple electronic states with multiple transition dipole moments and acts as a randomized donor. This multiplicity is not affected even in the absence of rotational motion and eliminates the problem of the orientation factor, particularly for cTnC immobilized in its complexes with the other two subunits. The distributions of the distances are narrower in the complexes, but the half-widths of the distributions still suggest some conformational dynamics of cTnC in the assembly.

That the interdomain distance of cTnC is not altered in cTnC-cTnI or cTn suggests that cTnC remains elongated in the complexes regardless of whether the regulatory site is occupied. The elongated conformation of cTnC in the complexes is in agreement with results from NMR and spin labeling studies which suggested an interdomain flexibility in free Ca^{2+}-loaded cTnC (Kleerekoper et al., 1995), in qualitative agreement with the observed half-width of the distribution of the interdomain distances. The present results are also consistent with results from small-angle scattering studies of the $4Ca^{2+}$ state of fsTnC complexed with full-length skeletal TnI (Olah & Trewhella, 1994; Olah et al., 1994) and fsTnC complexed with skeletal TnI and TnT (Stone et al., 1998). The X-ray crystallographic structure of the complex formed between fsTnC and a skeletal TnI regulatory peptide (residues 1–47) showed a collapsed TnC structure with direct polar interactions between the N-domain and C-domain (Vassyley et al., 1998). This structure of the skeletal TnC-peptide complex is not consistent with the present FRET result obtained with full-length cTnI. A recent study of fsTnC in the absence and presence of a 21-residue skeletal TnI inhibitory peptide suggested that fsTnC with an apo N-domain within the troponin complex would be spherical, but would become elongated when the regulatory sites in the N-domain were saturated (Moncrieffe et al., 1999). Our results do not support such a large scale conformational transition of cTnC within cTn induced by occupation of the single regulatory site. There are substantial conformational differences in the regulatory N-domain between cTnC and fsTnC (Sia et al., 1997; Dong et al., 1999). cTnI has a unique 33-residue extension at the N-terminus, and this extension and other structural features may make it difficult to directly compare the cardiac and skeletal systems without additional studies at this time. On the other hand, the skeletal TnI inhibitory peptide has a propensity to interact independently with the two TnC domains (Nagi & Hodges, 1992; Swenson & Frederickson, 1992). Such interaction would bring the two domains close to each other in the fsTnC-peptide complex, giving rise to a highly symmetric hydrodynamic shape. The antiparallel orientation of cTnC and cTnI in their binary complex (Farah et al., 1994) likely provides an anchor to maintain an elongated conformation of TnC in the complex. This possibility is supported by the findings that the interdomain distance of free cTnC is reduced by 6 Å when the regulatory site in the N-domain is occupied, but the distance is lengthened when the cTnC is bound to the other two subunits. The binding of activator Ca^{2+} does not induce a large opening of the N-domain in cTnC as it does in fsTnC (Sia et al., 1997; Dong et al., 1999), unless cTnC is bound to cTnI (Dong et al., 1999). If the Ca^{2+}-induced domain opening is dependent upon an optimal elongation of cTnC, then a role of bound cTnI would be to maintain the interdomain separation to enhance domain opening, thus allowing cTnI to interact with an exposed hydrophobic pocket in cTnC.

No high resolution data are yet available on the shape and dimensions of the cardiac troponin complex. An early low-resolution study by rotatory shadowing revealed a bipartite structure of the skeletal troponin complex with a total length of 265 nm, where TnC and TnI form a globular domain and TnT forms a long tail-like structure (Flicker et al., 1982). A similar structure is not available for cardiac troponin. Assuming that the global topography is similar for the two isoforms, FRET results suggest that a minimal dimension of the globular domain of cardiac troponin is in the range of 50 Å. This information and the results from intersubunit distances will allow topographic mapping of cTn including the long tail of its cTnT partner.

In summary, we have determined an interdomain distance in cTnC using tryptophan-sensitized luminescence of Tb^{3+} bound to site III as the energy donor. This sensitization eliminates simultaneous excitation of Tb^{3+} bound to other sites. The results suggest that cTnC has a similar elongated shape whether it is isolated in solution or within the troponin complex and that occupation of the regulatory site does not result in an apparent perturbation of this elongation in the troponin complex. While isolated cTnC has considerable conformational dynamics between the two domains, it does not appear highly immobilized when complexed with cTnI or cTnI and cTnT. The elongated interdomain dimension and the reduced conformational dynamics of cTnC in cTn may be a structural basis to allow for insertion of a segment of cTnI into the open regulatory N-domain upon Ca^{2+} activation.

Materials and methods

Protein preparations

Cardiac TnC mutants Y111W and R147W were genetically generated from a chicken slow muscle TnC cDNA clone as previously outlined and using a PCR kit (Dong et al., 1999). These mutants contained an additional mutation in which Cys84 was replaced by Ser, leaving the other endogenous Cys35 in place. The single cysteine was labeled with IAATMR (Research Organics, Cleveland, Ohio) under denatured conditions (Dong et al., 1996), and unreacted free probe was removed using a DEAE-Sephadex A-50 column equilibrated with a buffer containing 6 M urea, 20 mM imidazole at pH 7.0, 1 mM EDTA, and 0.1 mM DTT. Labeled proteins were eluted with a linear gradient formed by 500 mL of the column buffer and 500 mL of the buffer containing 0.5 M KCl. The eluted proteins were dialyzed against a buffer consisting of 50 mM MOPS at pH 6.9 and 100 mM KCl (buffer A)and 10 μM EGTA, which was prepared with Chelex 100 resin-treated deionized and distilled water. The degree of -SH labeling was deter-

mined to be >95% for both single-tryptophan mutants. The cTnC mutants were tested for their ability to confer Ca^{2+} sensitivity in a myofibrillar ATPase assay (Dong et al., 1999). Recombinant cTnI was prepared from a mouse cDNA clone as in previous work (Dong et al., 1997b), and native cTnT was prepared from bovine heart (Dong et al., 1997c). The binary complex cTnC-cTnI and fully reconstituted cTn were obtained with cTnC mutant Y111W, recombinant wild-type cTnI, and native cTnT as previously described (Dong et al., 1997c).

Fluorescence spectroscopy

Steady-state measurements were carried out on an ISS PC1 spectrofluorometer at 20 ± 0.1 °C. The band pass of both the excitation and emission monochromators was set at 3 nm. Emission spectra were corrected for variations of the detector system with wavelengths. Fluorescence quantum yields of the tryptophan residues were determined by the comparative method as in previous work (She et al., 1998). A standard calcium solution (Orion) was used in Ca^{2+} titration experiments, using EGTA to control the Ca^{2+} level and known stability constants of the chelator for proton and cations to calculate free Ca^{2+} concentration (Dong et al., 1997d).

Time-resolved measurements of the decays of both tryptophan and Tb^{3+} were made on an IBH 5000 photon-counting lifetime system equipped with different excitation sources. For the intensity decay of tryptophan, a very stable nanosecond flash lamp was used at 40,000 Hz in 0.5 atm of hydrogen; the excitation wavelength was 295 nm. For the decay of Tb^{3+} intensity sensitized by tryptophan, a 100 Hz xenon flash lamp (120 ns full width at half maximum and 5 mJ of pulse energy) was used as the excitation source, with the excitation wavelength at 295 nm and the sensitized Tb^{3+} luminescence detected at 545 nm. A low pressure pulsed nitrogen-pumped dye laser (Oriel #79110) with a dye (Oriel #79153) having an output at 479 nm was used for direct excitation of Tb^{3+}, and the Tb^{3+} luminescence was detected at 545 nm. Emitted photons were collected at 10 μs/channel after an 80 μs delay. A nonlinear least-squares iterative reconvolution procedure was used to recover the decay parameters from a sum of exponential terms. The goodness of fit was evaluated by the reduced chi-squares ratio (χ_R^2), the weighted residuals, and the Durbin–Watson parameter (D-W). In the experiments reported here, $0.9 < \chi_R^2 < 1.2$ and D-W > 1.8. The quantum yield of Tb^{3+} bound to cTnC was assumed to be 1.0 in 100% D_2O (Selvin & Hearst, 1994), and the quantum yield of bound Tb^{3+} in water (Q) was calculated from

$$Q = \tau(H_2O)/\tau(D_2O) \tag{1}$$

where τ is the lifetime of bound Tb^{3+} in H_2O or D_2O. For this determination, the decay time was measured at 545 nm with direct excitation.

Luminescence resonance energy transfer from bound Tb^{3+} to AATMR attached to Cys35 was determined from the luminescence intensity decay of the donor (Tb^{3+}) with two samples, one containing donor alone and the other containing both the donor and acceptor at Cys35. As a result of energy transfer, the donor decay was quenched in the presence of the acceptor. The donor decay would contain a small contribution from unquenched bound donor if the acceptor labeling was less than stoichiometric. To minimize this potential problem, we also measured the decay of the sensitized acceptor (AATMR) emission at 565 nm at which the background signal from the sharp 545 nm Tb^{3+} band is negligible. With an 80 μs delay, any AATMR emission arising from direct excitation (decay time nanoseconds) would have decayed away and only the sensitized AATMR emission due to an energy transfer between bound Tb^{3+} and the acceptor was detected. Under these conditions, the only species that contributed to the sensitized AATMR signal was from the donor-acceptor pair.

The donor luminescence decay data were used to calculate the distribution of the distances between the bound Tb^{3+} and AATMR-labeled Cys35. Briefly, the distance-dependent donor decay of a donor-acceptor pair separated by a given distance r is given by

$$I_{DA}(r,t) = \sum_i \alpha_{Di} \exp\left[-\frac{t}{\tau_{Di}} - \frac{t}{\tau_{Di}}\left(\frac{R_o}{r}\right)^6\right] \tag{2}$$

where τ_{Di} is the decay time for the donor in the absence of acceptor, α_{Di} is the associated amplitude, and R_o is the Förster distance at which the transfer is 50%. The observed decay for an ensemble of donor-acceptor pairs is given by

$$I_{DA}(t) = \int_0^\infty P(r) I_{DA}(r,t)\, dr \tag{3}$$

where $P(r)$ is the probability distribution of distances and is assumed to be a Gaussian function with the mean distance $\bar{r}$ and half-width $hw = 2.354\sigma$, where σ is the standard deviation of the distribution. The distribution was calculated from Equation 3 using the program CFS_LS/GAUDIS as in previous work (Dong et al., 1997a).

Acknowledgments

This work was supported in part by National Institutes of Health Grants HL52508 and RR10404.

References

Chabbert M, Lukas TJ, Watterson DM, Axelsen PH, Prendergast FG. 1991. Fluorescence analysis of calmodulin mutants containing tryptophan: Conformational changes by calmodulin-binding peptides from myosin light kinase and protein kinase II. *Biochemistry 30*:7615–7630.

Dong W-J, Chandra M, Xing J, She M, Solaro RJ, Cheung HC. 1997a. Phosphorylation-induced distance change in a cardiac muscle troponin I mutant. *Biochemistry 36*:6754–6762.

Dong W-J, Chandra M, Xing J, Solaro RJ, Cheung HC. 1997b. Conformation of the N-terminal segment of a monocysteine mutant of troponin I from cardiac muscle. *Biochemistry 36*:6745–6753.

Dong W-J, Rosenfeld SS, Wang C-K, Gordon AM, Cheung HC. 1996. Kinetic studies of calcium binding to the regulatory site of troponin C from cardiac muscle. *J Biol Chem 271*:688–694.

Dong W-J, Wang C-K, Gordon AM, Cheung HC. 1997c. Disparate fluorescence properties of 2-[4′-(iodoacetamido)anilino]-naphthalene-6-sulfonic acid attached to Cys-84 and Cys-35 of troponin C in cardiac muscle troponin. *Biophys J 72*:850–857.

Dong W-J, Wang C-K, Gordon AM, Rosenfeld SS, Cheung HC. 1997d. A kinetic model for the binding of Ca^{2+} to the regulatory site of troponin from cardiac muscle. *J Biol Chem 272*:19229–19235.

Dong W-J, Xing J, Villian M, Hellinger M, Robinson JM, Chandra M, Solaro RJ, Umeda PK, Cheung HC. 1999. Conformation of the regulatory domain of cardiac muscle troponin C in its complexes with cardiac troponin I. *J Biol Chem 274*:31382–31390.

Farah CS, Miyamoto CA, Ramos CHI, da Silva ACR, Quaggio RB, Fujimori K, Smillie LB, Reinach FC. 1994. Structural and regulatory functions of the NH_2- and COOH-terminal regions of skeletal muscle troponin I. *J Biol Chem 269*:5230–5240.

Flicker PF, Phillips GN, Cohen C. 1982. Troponin and its interaction with tropomyosin. *J Mol Biol 162*:495–501.

Herzberg O, James MNG. 1985. Structure of the calcium regulatory protein troponin-C at 2.8 Å resolution. *Nature 313*:653–659.

Horrocks WD Jr, Collier WE. 1981. Lanthanide ion luminescence probes. Measurement of distance between intrinsic protein fluorophores and bound metal ions: Quantitation of energy transfer between tryptophan and terbium (III) or europium (III) in the calcium-binding protein parvalbumin. *J Am Chem Soc 103*:2856–2862.

Horrocks WD Jr, Sudnick DR. 1979. Lanthanide ion probes of structure in biology. Laser-induced luminescence decay constants provide a direct measure of the number of metal-coordinated water molecules. *J Am Chem Soc 101*:334–340.

Kanellis P, Yang J, Cheung HC, Lenkinski RE. 1983. Synthetic peptide analogs of skeletal troponin C: Fluorescence studies of analogs of the low-affinity calcium-binding site II. *Arch Biochem Biophys 220*:530–540.

Kleerekoper Q, Howarth JW, Guo X, Solaro RJ, Rosevear PR. 1995. Cardiac troponin I induced conformational changes in cardiac troponin C as monitored by NMR using site-directed spin and isotope labeling. *Biochemistry 34*:13343–13352.

Lakowicz JR, Gryczynski T, Cheung HC, Wang C-K, Johnson ML, Joshi N. 1988. Distance distributions in proteins recovered by using frequency-domain fluorometry. Application to troponin I and its complex with troponin. *Biochemistry 27*:9149–9160.

Leavis PC, Nagy B, Lehrer SS, Bialkowske H, Gergely J. 1980. Terbium binding to troponin C: Binding stoichiometry and structural changes induced in the protein. *Arch Biochem Biophys 200*:17–21.

MacManus JP, Hogue CW, Mardsen BH, Sikorska M, Szabo AG. 1990. Terbium luminescence in synthetic peptide loops from calcium-binding proteins with different energy donors. *J Biol Chem 265*:10358–10366.

Malik NA, Anantharamaiah GM, Gawish A, Cheung HC. 1987. Structural and biological studies on synthetic peptide analogues of a low-affinity calcium-binding site of skeletal troponin C. *Biochim Biophys Acta 911*:221–230.

Moncrieffe MC, Eaton S, Bajzer Z, Haydock C, Potter JD, Laue TM, Prendergast FG. 1999. Rotational and translational motions of troponin C. *J Biol Chem 274*:17464–17470.

Nagi S-M, Hodges RS. 1992. Biologically important interactions between synthetic peptides of the N-terminal region of troponin I and troponin C. *J Biol Chem 267*:15715–15720.

Olah GA, Rokop SE, Wang C-LA, Blechner SL, Trewhella J. 1994. Troponin I encompasses an extended troponin C in the Ca^{2+}-bound complex: A small-angle X-ray and neutron scattering study. *Biochemistry 33*:8233-8239.

Olah GA, Trewhella J. 1994. A model structure of the muscle protein complex $4Ca^{2+}$·troponin C·troponin I derived from small-angle scattering data: Implications for regulation. *Biochemistry 33*:12800–12806.

Selvin PR, Hearst JE. 1994. Luminescence energy transfer using a terbium chelate: Improvement on fluorescence energy transfer. *Proc Natl Acad Sci USA 91*:10224–10228.

Sia SK, Li MX, Spyracopoulos SM, Gagné W, Liu W, Putkey JA, Sykes BD. 1997. Structure of cardiac muscle troponin C unexpectedly reveals a closed regulatory domain. *J Biol Chem 272*:18216–18221.

She M, Xing J, Dong W-J, Umeda PK, Cheung HC. 1998. Calcium binding to the regulatory domain of skeletal muscle troponin C induces a highly constrained open conformation. *J Mol Biol 281*:445–452.

Stone DB, Timmins PA, Schneider DK, Krylova I, Ramos CHI, Reinach FC, Mendelson RA. 1998. The effect of regulatory Ca^{2+} on the in situ structures of troponin C and troponin I: A neutron scattering study. *J Mol Biol 281*:689–704.

Sundaralingam M, Bergstrom R, Strasburg RT, Rao P, Roychowdhury P, Greaser M, Wang B-C. 1985. Molecular structure of troponin C from chicken skeletal muscle at 3 Å resolution. *Science 227*:945–948.

Swenson CA, Frederickson RS. 1992. Interactions of troponin C and troponin C fragments with troponin I and the troponin I inhibitory peptide. *Biochemistry 31*:3420–3429.

Vassyley DG, Takeda S, Wakatsuki S, Maeda K, Maeda Y. 1998. Crystal structure of troponin C in complex with troponin I fragment at 2.3 Å resolution. *Proc Natl Acad Sci USA 95*:4847–4852.

Wang C-LA, Leavis PC. 1990. Distance measurements in cardiac troponin C. *Arch Biochem Biophys 276*:236–241.

Wang C-L, Leavis PC, Horrocks WW, Gergely J. 1981. Binding of lanthanide ions to troponin C. *Biochemistry 20*:2439–2444.

Wang C-LA, Tao T, Gergely J. 1982. The distance between the high affinity sites of troponin-C. Measurement of interlanthanide ion energy transfer. *J Biol Chem 257*:8372–8375.